Behavioral/Systems/Cognitive

Feedforward Inhibition of Projection Neurons by Fast-Spiking GABA Interneurons in the Rat Striatum *In Vivo*

Nicolas Mallet,[1] Catherine Le Moine,[1] Stéphane Charpier,[2] and François Gonon[1]

[1]Centre National de la Recherche Scientifique, Unité Mixte de Recherche 5541, Université Victor Segalen Bordeaux 2, 33076 Bordeaux, France, and [2]Institut National de la Santé et de la Recherche Médicale, Unité 114, Chaire de Neuropharmacologie, Collège de France, 75231 Paris, France

Discharge activities and local field potentials were recorded in the orofacial motor cortex and in the corresponding rostrolateral striatum of urethane-anesthetized rats. Striatal projection neurons were identified by antidromic activation and fast-spiking GABAergic interneurons (FSIs) by their unique characteristics: briefer spike and burst responses. Juxtacellular injection of neurobiotin combined with parvalbumin immunohistochemistry validated this identification. Spontaneous activities and spike responses to cortical stimulation were recorded during both states of cortical activity: slow waves and desynchronization. Both FSI and projection neurons spontaneously discharged synchronously with slow waves at the maximum of cortical activity, but, on average, FSIs were much more active. Cortical desynchronization enhanced FSI activity and facilitated their spike responses to cortical stimulation, whereas opposite effects were observed regarding projection neurons. Experimental conditions favoring FSI discharge were always associated with a decrease in the firing activity of projection neurons. Spike responses to cortical stimulation occurred earlier (latency difference, 4.6 ms) and with a lower stimulation current for FSIs than for projection neurons. Moreover, blocking $GABA_A$ receptors by local picrotoxin injection enhanced the spike response of projection neurons, and this increase was larger in experimental conditions favoring FSI responses. Therefore, on average, FSIs exert *in vivo* a powerful feedforward inhibition on projection neurons. However, a few projection neurons were actually more sensitive to cortical stimulation than FSIs. Moreover, picrotoxin, which revealed FSI inhibition, preferentially affected projection neurons exhibiting the weakest sensitivity to cortical stimulation. Thus, feedforward inhibition by FSIs filters cortical information effectively transmitted by striatal projection neurons.

Key words: **basal ganglia; striatum; GABAergic; interneuron; parvalbumin; spiny neuron**

Introduction

The striatum is a main input structure of the basal ganglia and receives massive glutamatergic cortical inputs from all functional subdivisions of the neocortex (Gerfen and Wilson, 1996; Bolam et al., 2000). This cortical information is integrated in the striatum and generates activities that finally disinhibit premotor nuclei in the thalamus and brainstem. Because striatal neuronal activity is involved in learning, reward expectation, and movement preparation (Graybiel, 1995; Schultz et al., 2003), the understanding of how cortical information is processed in the striatum is of fundamental importance.

A frontal electroencephalogram exhibits two states in urethane-anesthetized rats: the first one is characterized by slow waves of large amplitude at a frequency close to 1 Hz, and the second, often called "cortical desynchronization," is characterized by the absence of slow waves. Both states resemble electroencephalogram patterns recorded during slow-wave sleep and alertness, respectively (Steriade, 2000). In the striatum, medium-size spiny neurons (MSNs) represent 90% of the neuronal population. Their membrane potential oscillates between a hyperpolarized "down" state and a depolarized "up" state. Initiation and maintenance of the up state require excitatory cortical inputs (Wilson, 1993; Wilson and Kawaguchi, 1996; Stern et al., 1997). During cortical slow waves in anesthetized rats, the synchronous activity of corticostriatal neurons actually shapes the membrane potential of MSNs (Mahon et al., 2001; Tseng et al., 2001). These oscillations are disrupted by cortical desynchronization (Mahon et al., 2001; Kasanetz et al., 2002).

MSNs are GABAergic and project either to the pallidum or to the substantia nigra pars reticulata (SNr) (Gerfen and Wilson, 1996). The remaining striatal neurons are cholinergic and GABAergic interneurons (Kawaguchi, 1993; Kawaguchi et al., 1995). Because MSNs and GABAergic interneurons are interconnected in highly organized microcircuitry and communicate via GABAergic synapses, local GABA inputs may modulate the excitability of MSNs (Calabresi et al., 1990, 1991; Nisenbaum and Berger, 1992; Kita, 1993, 1996). Despite the density of local collateral axons originating from MSNs (Bolam et al., 2000), lateral inhibition between MSNs appears functionally weak (Kita 1993; Jaeger et al., 1994) and might play a role only during repetitive activation (Plenz, 2003). Instead, *in vitro* studies (Kita, 1996;

Received Sept. 30, 2004; revised Feb. 22, 2005; accepted March 1, 2005.

This work was supported by the Centre National de la Recherche Scientifique, the Université Victor Segalen Bordeaux 2, and the Ministère Français de la Recherche (Action Concertée Incitative "Biologie du Développement et Physiologie Intégrative" 2002). We thank Prof. Jean-Michel Deniau, who gave a decisive impetus to this study, and Drs. Richard Miles and Kuei Y. Tseng for thoughtful discussion and critical reading of this manuscript.

Correspondence should be addressed to François Gonon, Centre National de la Recherche Scientifique, Unité Mixte de Recherche 5541, Boîte Postale 28, Université Victor Segalen Bordeaux 2, 33076 Bordeaux, France. E-mail: francois.gonon@umr5541.u-bordeaux2.fr.

DOI:10.1523/JNEUROSCI.5027-04.2005

 0270-6474/05/253857-13$15.00/0

Plenz and Kitai, 1998; Koos and Tepper, 1999) suggest that striatal GABAergic inhibition mainly derives from fast-spiking interneurons (FSIs), a subclass of GABAergic interneurons containing parvalbumin (Cowan et al., 1990; Kita et al., 1990; Kawaguchi, 1993). In accordance with this view, parvalbumin-positive neurons receive direct cortical inputs (Kita et al., 1990; Bennett and Bolam, 1994; Ramanathan et al., 2002), form symmetrical synapses on somata and proximal dendrites of MSNs (Bennett and Bolam, 1994), and are easily activated by cortical stimulation (Parthasarathy and Graybiel, 1997). However, the discharge activity of identified FSIs has not yet been studied *in vivo*. In the present study, we have characterized FSI activity and have shown that the cortex exerts, via FSIs, a potent feedforward inhibition on MSNs *in vivo*. Because striatal integration of cortical inputs may depend on the pattern of cortical activity, we investigated this inhibition during both cortical slow waves and desynchronization.

Materials and Methods

Animal preparation. Experiments were performed *in vivo* in accordance with French (87-848, Ministère de l'Agriculture et de la Forêt) and European Economic Community (86-6091) guidelines for care of laboratory animals. Sixty adult Sprague Dawley rats (330–430 g) were anesthetized with urethane administered at a dose (range, 1.2–1.67 g/kg, i.p.; mean ± SD, 1.35 ± 0.11 g/kg) sufficient to induce a complete loss of the righting reflex and abolition of any movement response to a tail pinch. Few rats, which did not meet these criteria with a dose superior to 1.7 g/kg, were discarded. During experiments, responses to a tail pinch were repeatedly tested. In a few cases in which a movement response reappeared, an additional dose of urethane (0.25 g/kg) was administered. Rats were fixed in a stereotaxic frame according to the atlas of Paxinos and Watson (1997) and maintained at 37°C with a homeothermic blanket. The skull was infiltrated with lidocaine (2%) before surgery.

Electrical stimulations. A concentric bipolar electrode (SNEX-100; Rhodes Medical Instruments, Summerland, CA) was implanted in the rostral part of the SNr, 2.4 mm lateral to the medial line, 4.8 posterior to bregma, and 8.0 mm below the cortical surface. The orofacial area of the motor cortex was stimulated with a bipolar electrode modified from a SNEX-200 electrode (Rhodes Medical Instruments); both exposed tips were parallel, 0.1 mm in diameter, 0.25 mm long, and 0.67 mm apart. This bipolar electrode was implanted in a sagittal plane 3.2 mm lateral to the medial line, 3.0 and 3.67 rostral to bregma, and 1.6 below the cortical surface. With both electrodes, a current pulse (0.5 ms long) was applied with an isolated stimulator (DS3; Digitimer, Hertfordshire, UK) triggered either by a MacLab/4S system (AD Instruments, Castle Hill, New South Wales, Australia) or a 1401 Plus system (Cambridge Electronic Design, Cambridge, UK).

Because most striatal neurons are silent, cortical stimulations at the maximal current used in the present study (600 μA) were continuously applied at 1 Hz while searching for striatal neurons. However, all further investigations regarding spike responses of individual neurons to paired cortical stimulation were performed at 0.33 Hz to avoid interference (e.g., short-term facilitation in the 1 Hz range) between successive paired stimulations.

Antidromic stimulation of the SNr was used to identify striatonigral neurons. Spike responses evoked by SNr stimulation were considered antidromic when they fulfilled the following criteria: (1) constant latency of spike response, (2) all-or-none property of the spike response when the strength of the stimulation was adjusted just above or just below threshold, and (3) collision of the antidromic spikes with orthodromic spikes. Because most striatal neurons are silent, the orthodromic spike required for the collision test was evoked by cortical stimulation, and the SNr stimulation was triggered by the spike evoked by cortical stimulation with a delay of 30 or 3 ms, alternately, as illustrated in Figure 1*A*. Collision had to be observed 10 times during a series of 10 successive tests to be considered positive. The stimulation current used in collision tests for antidromic stimulation of the 53 striatonigral neurons studied ranged from 70 to 600 μA. Striatal neurons were considered unresponsive to antidromic stimulation of the SNr either if their spike responses evoked by SNr stimulation did not meet the above-mentioned criteria or if they exhibited no spike response to SNr stimulation at maximal current (1 mA).

Antidromic stimulation of the contralateral striatum was used to identify corticostriatal neurons. Indeed, contralateral stimulation allowed us to avoid any antidromic stimulation of passing corticofugal axons (Wilson, 1987). For this purpose, a bipolar concentric electrode (SNEX-100; Rhodes Medical Instruments) was implanted in the contralateral striatum 3.1 mm lateral to the medial line, 1.2 rostral to bregma, and 4.75 mm below the cortical surface. Antidromic identification met the three criteria mentioned above. The current used for antidromic activation of the 14 corticostriatal neurons studied ranged from 130 to 900 μA.

Spike recording. Single-cell extracellular recordings were performed with glass pipette pulled from glass capillaries (GC150F; Harvard Apparatus, Edenbridge, UK) using a Pull 1 puller (WPI, Hertfordshire, UK). The pulled tip of the pipette was broken under a microscope at an external diameter of 1.2–1.4 μm. Pipettes were filled with 1% neurobiotin (Vector Laboratories, Burlingame, CA) dissolved in 0.4 M NaCl. Their resistance was measured *in vivo* with an Axoclamp2B (Axon Instruments, Foster City, CA) by bridge balance and was found to be ~18 MΩ (range, 13–24 MΩ). These electrodes were implanted in the lateral part of the rostral striatum 3.0–3.4 mm to the medial line, 1.0–1.3 mm rostral to bregma, and 3.5–5.8 mm below the cortical surface. Some neurons were also recorded in the orofacial motor cortex between 1.0 and 2.0 mm below the cortical surface. Through these electrodes, the extracellular potential was recorded with an Axoclamp2B amplifier in the bridge mode versus a reference electrode maintained in contact with the skull by a sponge moistened with a 0.9% NaCl solution. The extracellular potential amplified 10 times and filtered at 10 kHz by the Axoclamp2B amplifier was further amplified 100 times via two distinct channels of a differential AC amplifier (model 1700; A-M Systems, Carlsborg, WA). One channel was used for spike recording (low-pass filter at 300 Hz and high-pass filter at 10 kHz), and the other channel (low-pass filter at 0.1 Hz and high-pass filter at 10 kHz) was used to record the local field potential (see below). The output of the first channel was digitized at 20 kHz with a MacLab/4S system and recorded using the Scope program for detailed examination of every spike, including spikes evoked by electrical stimulation. The same output was also connected to a Window Discriminator (WPI) for spike detection. Spike occurrence was continuously recorded by a 1401 Plus Cambridge Electronic Design system running Spike 2.

Field potentials. Field potentials were recorded in the orofacial motor cortex either with the most caudal tip of the stimulating electrode or with a carbon fiber electrode whose active surface was a single section of carbon fiber (7 μm in diameter). These electrodes were connected to an AC amplifier (P55; Grass-Telefactor, West Warwick, RI; 1000 times amplification, low-pass filter at 0.1 Hz and high-pass filter at 3 kHz). In the striatum, the field potential was recorded, as indicated above, through the glass pipette and the second channel of the differential amplifier. Both amplified field potentials were digitized at 1 kHz by the Cambridge Electronic Design system and displayed with a polarity chosen so that the maximum of the slow waves corresponded to the maximal activity in the cortex. Control experiments showed that the monitoring of a field potential through a glass pipette is a valid technique. Indeed, we compared cortical field potentials recorded simultaneously with a large electrode and with a glass pipette during the course of the experiment described in Figure 7*A1*. Slow waves recorded via the glass pipette were found to be highly correlated with those recorded in the same cortical area with larger electrodes (maximum of the correlation coefficient, 0.93 ± 0.04, mean ± SD; $n = 35$). However, slow waves recorded through the glass pipette appeared 6.0 ± 3.4 ms (35 determinations in 35 distinct recording sites from nine rats) after those recorded with larger electrodes.

Local injections of picrotoxin. Picrotoxin (Sigma, Saint-Quentin Fallavier, France) was injected in the vicinity of recorded neurons using a glass pipette glued 150 μm above the tip of the recording pipette. Injection pipettes were pulled from glass capillaries (Ringcaps; Hirschmann Laborgerate, Eberstadt, Germany), which allowed us to accurately measure each injected volume in the range of 10–30 nl by visual observation of the meniscus. The pulled tip of the injection pipette was broken under

a microscope at an external diameter of 30 μm. Stock solutions of picrotoxin (50 mM) were prepared in distillated water and stored at 5°C. Picrotoxin was diluted in physiological solution (9 g/l NaCl, 0.2 g/l KCl, and 132 mg/l $CaCl_2$-$2H_2O$) at a final concentration of 1 mM and injected (20–30 nl) by air pressure within 6–12 s under visual control. Between injections, the absence of meniscus movement showed that no spontaneous leakage occurred with this type of pipette. Pressure injection induced a mechanical effect, which usually induced a decrease in spike amplitude. In most cases, the spike amplitude recovered within 1 min. Therefore, the early effects of picrotoxin injection on the discharge activity of a recorded neuron, which occurred during the first minute after injection, were not considered. In most neurons, picrotoxin injection strongly facilitated the discharge activity, and this increase reached a plateau between 1 and 6 min after injection. Then, the discharge activity gradually recovered within 10–15 min. Therefore, the effects of picrotoxin were considered during a 5 min period starting 1 min after injection.

Juxtacellular injection of neurobiotin. A representative population of striatal neurons was labeled with neurobiotin as described by Pinault (1996). Briefly, positive current pulses (2–6 nA, 250 ms) were applied at 2 Hz. The current was slowly increased until it drove the discharge activity. Then, this rhythmic activity was maintained for 2–4 min. At the end of the experiment, to facilitate further histochemical observations, four injections of Pontamine sky blue (Interchim, Montlucon, France) were performed in a coronal plane 200 μm rostral to cells injected with neurobiotin. This dye was injected at a volume of 10 nl by air pressure using the same type of injection pipette as described above.

Immunohistochemical detection of neurobiotin together with parvalbumin. After electrophysiological recordings, rats were perfused through the heart with 30 ml of saline (9% NaCl) and then with 200 ml of 4% paraformaldehyde. After perfusion, brains were dissected out and kept overnight in 4% paraformaldehyde. Vibratome sections (40 μm thick) were collected in PBS and then transferred in PBS and 30% sucrose for 1 h. Each well contained all sections from one rat starting from the blue landmarks and going up to 1 mm further posterior. Thus, 20–25 sections were collected to cover the entire area of interest. Before immunohistochemistry, to facilitate penetration of the antibodies, sections were flash-frozen in isopentane at −40°C and then immediately transferred again in PBS.

After 1 h of pretreatment in PBS, 0.3% Triton X-100, and 3% normal goat serum, free-floating sections were incubated overnight at room temperature under agitation with a combination of Alexa 568-conjugated streptavidin (1:800; Molecular Probes, Eugene, OR) and a monoclonal mouse anti-parvalbumin antibody (1:10,000; Swant) in PBS and 0.3% Triton X-100. After rinsing three times in PBS, the sections were incubated with an FITC-conjugated goat anti-mouse antibody for 90 min at room temperature (1:400 in PBS; Jackson ImmunoResearch, West Grove, PA), rinsed again three times for 10 min in PBS, and mounted in Vectashield for microscopic fluorescent observation (Axioplan 2; Zeiss, Oberkochen, Germany).

Data analysis. The field potential recorded in the cortex during periods of continuous slow waves lasting for at least 2 min was analyzed with fast Fourier transform; its power spectrum was built by the Spike 2 program as illustrated in Figure 5*B*. Slow waves simultaneously recorded in the cortex and striatum were compared with cross-correlation displayed by Spike 2, with the cortical wave as the reference wave, from recording periods of 30 s as illustrated in Fig. 5*C*. From these cross-correlograms, two parameters were measured: the maximum of the correlation coefficient and the time interval between that maximum and time zero. The discharge activity of single neurons was analyzed with interspike interval (ISI) histograms and autocorrelograms built by Spike 2 with a bin width of 4 ms. The temporal relationship between slow waves and spike discharges was shown for every individual neuron by averaging, using Spike 2, the field potential recorded from −1 to +1 s around every spike as illustrated in Fig. 7*A*. Continuous periods of slow waves, during which at least 10 spikes were recorded, were used to build these averaged field potentials. From these averaged recordings, the time interval between their maximum and time zero (corresponding to every spike) was measured for every single neuron. Paired and unpaired *t* tests were used for statistical comparisons except in one case: in Fig. 4, the difference in discharge rate of SNr− neurons did not reach statistical significance with the paired *t* test because of the large deviation between individual neurons, but did it with the nonparametric Wilcoxon paired test.

Results

Identification of striatal neurons

Parvalbumin-positive neurons form the most numerous class of GABAergic interneurons in the rat striatum (Kawaguchi et al., 1995; Wu and Parent, 2000). Moreover, the density of parvalbumin-positive neurons is higher in the lateral striatum than in its medial part (Cowan et al., 1990; Kita, 1993), and an opposite gradient was observed for GABAergic interneurons expressing calretinin (Figueredo-Cardenas et al., 1996). Consequently, we studied FSIs in the rostrolateral striatum.

The rostrolateral striatum receives massive cortical inputs mainly originating from the orofacial motor cortex (McGeorge and Faull, 1989; Deniau et al., 1996). Because most striatal neurons are silent, electrical stimulation of the orofacial cortex was used to detect silent neurons as reported by Mahon et al. (2001). MSNs are striatal projection neurons belonging to two populations of similar size: striatonigral neurons project to the SNr, whereas striatopallidal neurons project to the external part of the globus pallidus (Gerfen and Wilson, 1996). Fifty-three neurons were identified as striatonigral MSNs by antidromic activation of the SNr (Fig. 1*A*) (Ryan et al., 1986; Jaeger et al., 1994) and called SNr+. Seven neurons were identified as tonically active, presumably cholinergic, interneurons: they exhibited a continuous spontaneous activity at a frequency between 2 and 4 Hz and a relatively long action potential duration (Wilson et al., 1990). These seven neurons were not further considered in the present study. Twenty-seven FSIs were distinguished from other striatal neurons by their unique short-lasting action potential (Kawaguchi, 1993). Indeed, the duration of their extracellular action potential, measured as indicated in Figure 1*B*, appeared clearly shorter compared with all other striatal neurons recorded in the same experimental conditions (Fig. 1*C*). The 63 neurons that did not fall into the three categories defined above and that did not exhibit an antidromic response to SNr stimulation were called SNr−. It is likely that most of them were striatopallidal MSNs.

We report here on 27 FSIs among 150 striatal neurons studied (Fig. 1). Obviously, this represents an overestimate of the FSI population, which is attributable to the fact that, in most experiments, we started to look at one FSI before studying other striatal neurons. However, in some other experiments ($n = 15$, including seven preliminary experiments), we considered without any selection all neurons, which were detected by cortical stimulation or were spontaneously active. In these unbiased experiments, we found six FSIs and five tonically active neurons among 98 striatal neurons. Therefore, the percentage of FSIs in the lateral striatum seems to be slightly higher than that of presumably cholinergic interneurons. However, the real percentage of FSIs among all striatal neurons cannot be inferred from our study because we ignored silent neurons unresponsive to cortical stimulation. According to Luk and Sadikot (2001), 0.7% of the striatal neurons are parvalbumin-positive.

Another unique characteristic of FSIs was their capability of responding with a high-frequency train (three to five action potentials) to suprathreshold cortical stimulation. In contrast, all other striatal neurons usually responded to cortical stimulation with a single spike and rarely with a doublet. This unique property was studied in detail in six FSIs (Fig. 2). The number of spikes evoked by every individual cortical stimulation was increased by increasing stimulating current above threshold (Fig. 2*B*). Inside

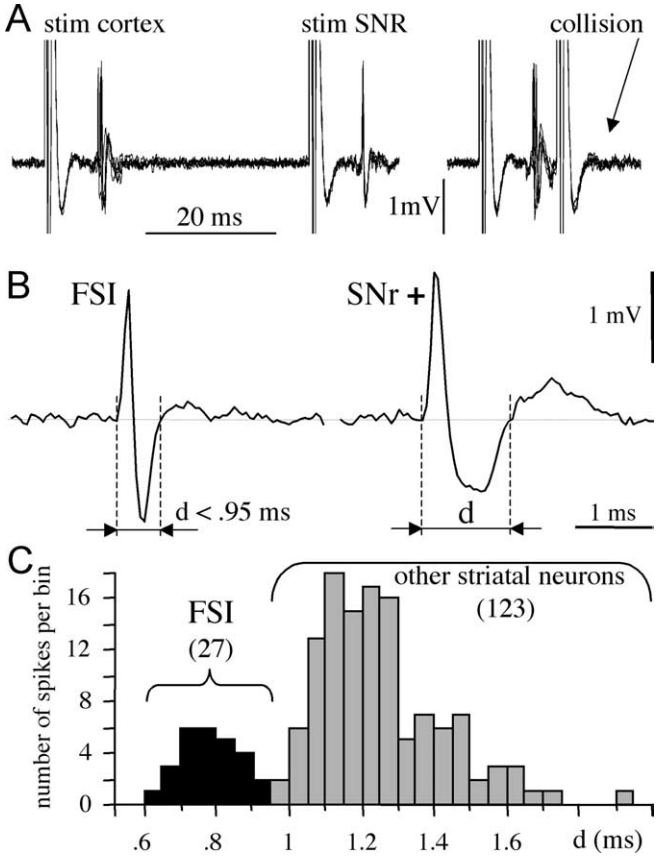

Figure 1. Electrophysiological identification of striatal neurons. ***A***, Example of a collision test used to identify a striatonigral neuron by antidromic activation of the SNr. The SNr stimulation (stim) was triggered by an orthodromic spike evoked by cortical stimulation either with a delay of 30 ms (no collision) or with a delay of 3 ms leading to collision of both spikes. Overlays of six consecutive recordings are shown. Notice that the antidromic spike evoked by SNr stimulation exhibited a fixed latency. ***B***, Examples of action potentials recorded either in one FSI (left) or in one SNr+ neuron (right) in the same animal. The action potential duration (d) was measured as indicated. ***C***, Distribution of the value of d (bin size, 5 ms). This value was below 0.95 ms for the 27 FSIs studied and superior to 0.95 ms regarding the 123 other striatal neurons. Spike duration discriminates FSIs from other striatal neurons.

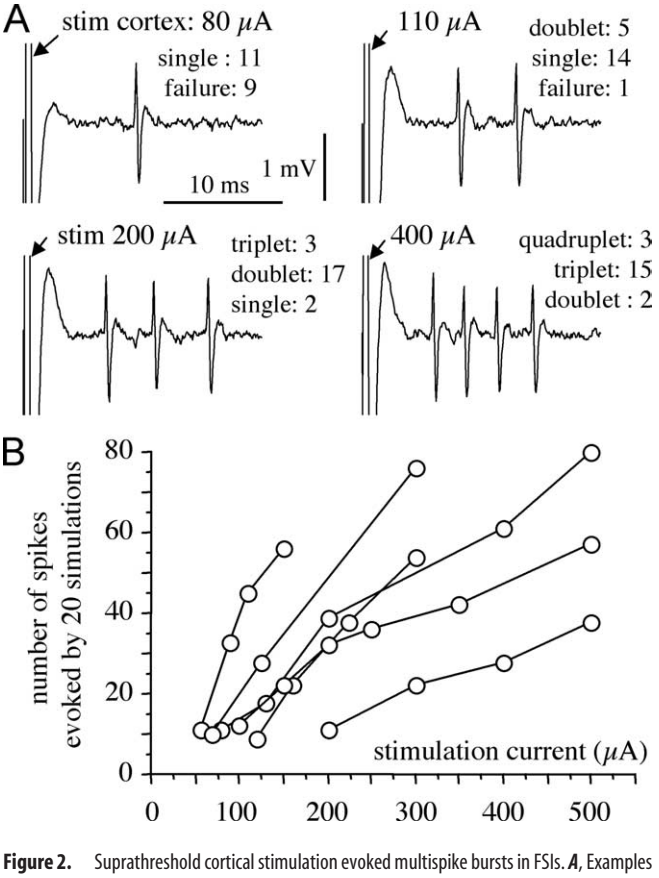

Figure 2. Suprathreshold cortical stimulation evoked multispike bursts in FSIs. ***A***, Examples of spike responses of one FSI to four series of 20 consecutive cortical stimulations (stim) at increasing currents. ***B***, Relationship between the stimulating current and the whole number of spikes evoked by series of 20 cortical stimulations (6 FSIs studied in 6 rats during the SW− state). This burst response consisting of three to five spikes represents a unique property of all FSIs.

Table 1. ISIs observed in bursts evoked in six FSIs by suprathreshold cortical stimulation

ISI	Doublet	Triplet	Quadruplet
1st (ms)	4.41 ± 1.16	3.27 ± 0.45	2.81 ± 0.20
2nd (ms)		3.55 ± 0.36	2.72 ± 0.45
3rd (ms)			3.64 ± 0.77
Mean (ms)	4.41 ± 1.16	3.41 ± 0.42	3.06 ± 0.66

As illustrated in Figure 2, cortical stimulation at increasing current evoked multispike responses. ISIs are expressed as mean ± SD. In quadruplets, the intraburst frequency reached 327 Hz.

these evoked bursts, the intraburst frequency was positively correlated to the number of spikes and exceeded 300 Hz (Table 1).

Representative populations of FSIs and MSNs were labeled with juxtacellular injection of neurobiotin. Double immunohistochemistry was performed to determine whether these injected neurons were also positive for parvalbumin. All five neurons successfully labeled with neurobiotin and previously identified as FSIs on the basis of their electrophysiological properties were found to be positive for parvalbumin (Fig. 3*A*,*C*). In contrast, all six MSNs (three SNr+ and three SNr−) successfully labeled with neurobiotin were found to be negative for parvalbumin (Fig. 3*B*,*D*).

Spontaneous activity of striatal and corticostriatal neurons

The cortical field potential exhibited two spontaneous states in rats anesthetized with urethane: a dominant state characterized by slow waves (SWs) of large amplitude at ~1 Hz, called here SW+ state, and periods of absence of slow waves (called here SW− state) (Tseng et al., 2001; Kasanetz et al., 2002). As observed by Kasanetz et al. (2002), a tail pinch always disrupted the slow-wave activity for a variable duration (Fig. 4). Several tail pinches applied for 5–10 s usually promoted an SW− state, which lasted for several minutes (Fig. 4). Moreover, in most rats, an SW− state also spontaneously occurred with a variable interval in the range of 20–90 min (data not shown). No differences were observed between a spontaneously occurring SW− state and a tail pinch-induced SW− state regarding all characteristics examined here (spontaneous discharge activity and spike response to cortical stimulation).

Fourteen corticostriatal neurons were recorded in the orofacial motor cortex and identified by antidromic stimulation of the contralateral striatum. These neurons did not show any overt response to a tail pinch (Fig. 4). On average, they exhibited similar discharge rates during both states: some neurons were more active during the SW− state (Fig. 4), whereas some others were less active (data not shown). In contrast, all 27 FSIs recorded in the striatum responded to a tail pinch with a prominent burst of action potentials (Fig. 4). Moreover, FSIs were much more active during the SW− state (Fig. 4). Obviously, burst responses of FSIs

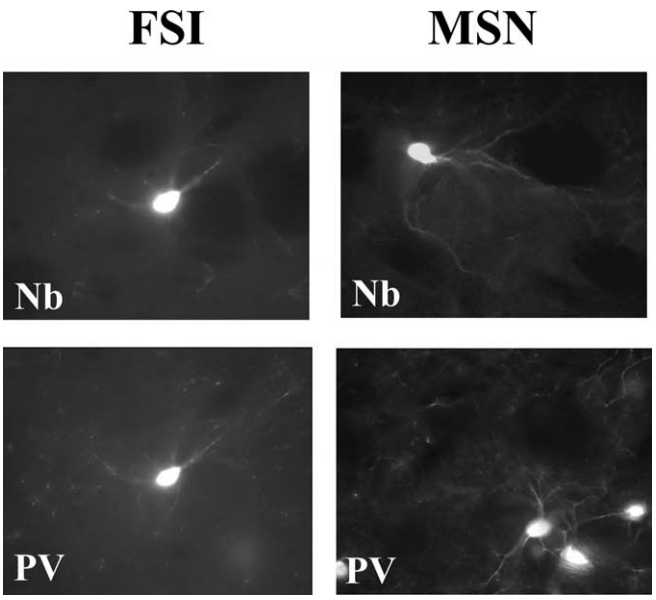

Figure 3. Immunohistochemical identification of FSI. A representative population of striatal neurons was labeled with neurobiotin by juxtacellular injection. FSIs labeled with neurobiotin were also immunoreactive for parvalbumin (left, 5 cells), whereas labeled MSNs were not (right, 6 cells). Nb, Neurobiotin; PV, parvalbumin.

to a tail pinch and their higher activity during the SW− state did not originate from the orofacial motor cortex and should involve other cortical and/or subcortical structures. In agreement with previous observations (Wilson, 1993), most SNr+ (22 of 31) and SNr− (24 of 34) neurons were silent during both states (discharge rate below 0.02 Hz during recording periods of at least 4 min in both states). Tail pinch never induced spikes in SNR+ neurons ($n = 53$) and in all but 4 SNR− neurons ($n = 63$). In all nine SNr+ neurons exhibiting low activity during the SW+ state (0.02–0.12 Hz), a tail pinch induced a silent period. These neurons were also less active during the SW− state (Fig. 4). Likewise, 10 SNr− neurons exhibiting moderate activity during the SW+ state (0.02–1.11 Hz) were silenced by a tail pinch (Fig. 4) and were also less active during the SW− state (Fig. 4). Finally, 4 of the 63 SNr− neurons were found to respond repeatedly with a burst to a tail pinch. These positive responses were observed in four distinct rats in which at least another SNr− neuron actually exhibited the typical negative response to a tail pinch. Therefore, these positive responses were not attributable to differences in experimental conditions. Among these four atypical SNr− neurons, three were very active during the SW− state (0.41, 3.03, and 7.66 Hz). Therefore, we reached the conclusion that these 4 SNr− neurons might belong to a distinct, unidentified class of neurons, and they were not further considered in this study. We assumed that most of the 59 remaining SNr− neurons were striatopallidal MSNs.

In most anesthetized preparations, the intracellular potential of MSNs oscillates at a frequency close to 1 Hz between a hyperpolarized down state and a depolarized up state. These oscillations are correlated with the rhythmic activity of corticostriatal neurons and the resulting cortical field potential (Mahon et al., 2001; Tseng et al., 2001; Kasanetz et al., 2002). Accordingly, we observed that the field potential recorded in the orofacial motor cortex exhibited slow waves of large amplitude at ~1 Hz (Fig. 5). Indeed, fast Fourier analysis of cortical field potential recorded during the SW+ state showed a prominent peak value at 1.09 ± 0.16 Hz (mean ± SD; 65 determinations in 27 animals) in the power spectrum of the signal (Fig. 5*B*). In 13 animals, both cortical and striatal field potentials were recorded simultaneously during the SW+ state. As illustrated in Figure 5*A*, both field potentials oscillated in a close temporal relationship. Cross-correlograms exhibited a maximal correlation coefficient close to 1 (0.87 ± 0.06, mean ± SD; 35 determinations in 35 distinct striatal recording sites, 13 rats) (Fig. 5*C*). However, the striatal waves appeared with an apparent delay of 17.0 ± 7.9 ms (mean ± SD; 35 determinations in 35 distinct striatal recording sites, 13 rats) (Fig. 5*C*). Taking into account the instrumental delay of 6.0 ms attributable to differences in recording techniques (see Materials and Methods), striatal slow waves followed cortical slow waves with a delay of 11 ms. It has been demonstrated in the nucleus accumbens of anesthetized rats that the slow waves of the local field potential reflect the rhythmic oscillations of the membrane potential between up and down states (Goto and O'Donnell, 2001). We assume that this is also the case in the striatum.

The pattern of spontaneous discharge activity was analyzed in detail for 8 FSIs and 10 MSNs (Fig. 6). During the SW+ state, both neuronal types discharged synchronously with the slow waves either with single spikes or brief bursts. Indeed, ISI histograms and autocorrelograms showed a peak at short intervals and a decreased number of intermediate intervals (0.3–0.8 s range) (Fig. 6, Table 2). On average, MSNs were less active than FSIs, and this difference explains why the mean and SD of all ISIs are larger for MSNs than for FSIs (Table 2). However, when considering the ISIs inferior to 200 ms, an opposite difference was observed (Table 2). This suggests that the intraburst frequency was higher for MSNs than for FSIs. FSIs exhibited a more regularly distributed discharge pattern and a higher mean discharge rate during the SW− state than during the SW+ state (Figs. 4, 6; Table 2). However, ISI analysis showed that this was not attributable to an increase in the instantaneous frequency during the SW− state but to a blockade of the discharge activity during the SW+ state except during the maximum of the slow waves. Indeed, the mean of the ISIs inferior to 200 ms was actually higher during the SW− state than during the SW+ state (Table 2). Our observation that FSIs spontaneously discharged with single spikes or brief bursts in synchrony with the slow waves and more regularly during the SW− state is consistent with a recent study on the spontaneous activity of presumed FSIs in freely moving rats (Berke et al., 2004). However, the most frequent intraburst ISI reported by these authors (2 ms) was much shorter than that observed here during the SW+ state (24 ms) (Table 2). Our observations are more consistent with those of Plenz and Kitai (1998) in organotypic cultures. Nevertheless, we also observed a very short ISI (3 ms) inside bursts evoked by suprathreshold cortical stimulations (Fig. 2, Table 1). As also reported (Mahon et al., 2001), during the SW+ state, the 14 corticostriatal neurons tested discharged synchronously with the cortical field potential (Fig. 7*A1*). In contrast, during the SW− state, apart from four neurons that became silent, the other corticostriatal neurons exhibited a more regularly distributed pattern of activity similar to that of FSIs (data not shown).

During the SW+ state, the discharge activity of corticostriatal neurons exhibited a wide distribution centered at the maximum of the cortical field (Fig. 7). This distribution is expected because the cortical field potential is actually generated by the rhythmic cortical activity (Steriade, 2000; Mahon et al., 2001). The distribution of FSI activity also appeared relatively wide: FSIs discharged either before or after the maximum of the striatal wave (Fig. 7*B*). Nevertheless, the distribution was centered close to that

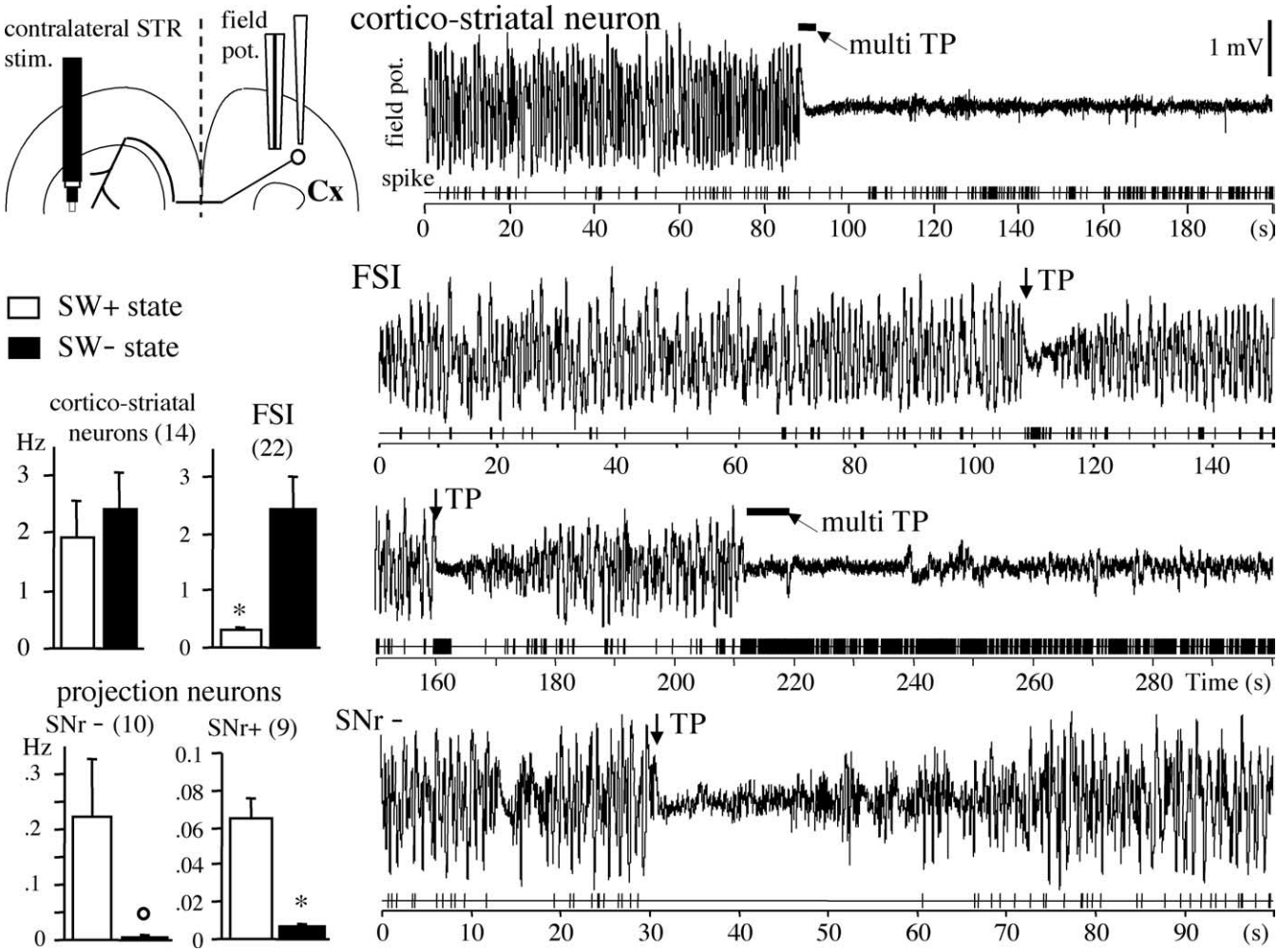

Figure 4. Spontaneous discharge activities of striatal neurons and corticostriatal neurons. Antidromic stimulation (stim.) of the contralateral striatum (STR) was used to identify corticostriatal neurons. Typical recordings show the cortical field potential recorded simultaneously with the discharge activity of one corticostriatal neuron (top traces), one FSI (both middle traces, continuous recording), and one SNr− neuron (i.e., presumed striatopallidal MSN, bottom traces). The cortical field potential exhibited either slow waves of high amplitude (SW+ state) or an absence of slow waves (SW− state). Indeed, with urethane anesthesia, the cortical field potential spontaneously oscillated between both states (data not shown). Moreover, a tail pinch (TP) disrupted the slow-wave activity. Only FSIs responded to a tail pinch with a train of action potential. Histograms indicate the mean discharge rate of four groups of neurons (numbers in parentheses) recorded for at least 4 min in both states. Silent MSNs are not included (see Results). Bar histograms indicate mean ± SEM (*$p < 0.001$; °$p < 0.01$; Wilcoxon test).

maximum (Fig. 7*D*). In contrast, the few active MSNs discharged in a more narrow way and 20.1 ms before the maximum of the striatal field potential, although this potential reflected the variations of the intracellular potential of MSNs. However, it must be pointed out that the discharge activity of MSNs was found to be extremely low if silent neurons were taken into account. Indeed, the 31 SNR+ and the 34 SNr− neurons recorded for at least 4 min during the SW+ state exhibited mean discharge rates of 0.019 and 0.078 Hz, respectively. In contrast, the 22 FSIs exhibited a mean discharge rate of 0.29 Hz. Therefore, the unexpected spike distribution of MSNs might represent the "surviving" spikes not inhibited by FSIs: when FSIs reached their maximal activity, MSNs became silent.

Spike responses to cortical stimulation

The relationship between the discharge probability of FSIs and the amplitude of the cortical stimulation was studied during both SW+ and SW− states (Fig. 8). All 11 FSIs tested were found to be much more responsive to cortical stimulation during the SW− state (Fig. 8*C*). In contrast, most MSNs (20/22 SNr+ and 22/23 SNr−) were less responsive during the SW− state. Most of them exhibited a spike probability that was so low during the SW− state that it was not possible to estimate the current necessary for a 50% probability within the current range used here (30–600 μA). On average, FSIs were found to be more responsive to cortical stimulation than MSNs during the SW+ state (Fig. 8*D*). However, the current necessary to induce a 50% spike probability in FSIs ranged from 125 to 350 μA (SD, 75 μA), whereas it ranged from 70 to 500 μA (SD, 121 μA) for MSNs. The higher variability of MSN sensitivity to cortical stimulation was observed both among experiments and among individual MSNs recorded in the same experiment. Therefore, a few MSNs were actually more responsive to cortical stimulation than FSIs during the SW+ state. We have recorded the discharge activity of 10 cortical neurons in the vicinity of our stimulating electrode (interelectrode distance, 0.7–1 mm). We observed that every stimulation completely inhibited the spontaneous discharge activity of each cortical neuron tested (data not shown). This inhibition lasted for 150–250 ms, i.e., for the same duration as the paired pulse inhibition of FSIs (Fig. 9).

When spike responses of FSIs were evoked by pairs of cortical stimulation, the response to the second pulse was found to be

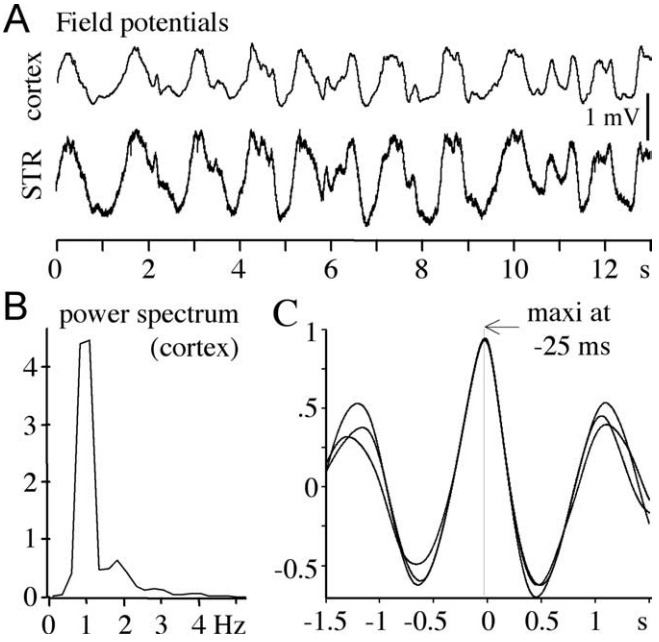

Figure 5. Temporal relationship between the field potentials recorded in the cortex and in the striatum during the SW+ state. ***A***, Field potentials were recorded simultaneously in the orofacial motor cortex with a large electrode and in the rostrolateral striatum (STR) with a glass pipette, which also recorded single-unit activity. ***B***, A power spectrum was built from field potentials recorded in the cortex during periods of a continuous SW+ state lasting for at least 2 min. ***C***, Cross-correlograms between the striatal field potential and the cortical field potential taken as the time references were built from a continuous period of an SW+ state lasting 30 s. maxi, Maximum. The three cross-correlograms exemplified in ***C*** corresponded to three periods obtained successively from the same continuous recording. Cross-correlograms show that the striatal field potential closely followed the cortical one with a delay of 11 ms (taking into account the instrumental delay; see Results).

strongly inhibited within intervals of 70–150 ms (Fig. 9). This characteristic was observed in both cortical states. Moreover, all 27 FSIs tested were more responsive to the first than to the second pulse, with an interval of 100 ms (data not shown). The discharge probability of FSIs was compared with that of MSNs in the same experiments by means of paired cortical stimulations (Fig. 10*A*). We observed that MSNs, in contrast to FSIs, were more responsive to the second pulse (Fig. 10*A*,*B*). Moreover, the discharge probability depended on the cortical state: the SW− state favored FSI responses to the first pulse and hindered that of MSNs. These reverse correlations suggest that FSIs inhibited MSN responses. Accordingly, the spike latency of FSIs was shorter when compared with that of MSNs, especially during the SW− state, wherein FSIs were highly responsive to cortical stimulation (Fig. 10*C*). The difference in spike latency between FSI and SNr+ neurons was 2.5 ms during the SW+ state and 4.6 ms during the SW− state. These differences were 2.4 and 4.1 ms regarding SNr− neurons. Whatever the conditions (first vs second pulse and SW+ versus SW− state), the spike response of MSNs always occurred with a relatively constant latency (12–13 ms), exhibiting a low variability (SD, <2.3 ms). Therefore, large changes in spike probability were not correlated with a major change in spike latency.

Effect of picrotoxin injection on the discharge probability of MSN

Blockade of $GABA_A$ receptors by pressure injection of picrotoxin in the vicinity of recorded MSNs facilitated their spike responses to paired cortical stimulations (Fig. 11). This facilitatory action was stronger for the first pulse (Fig. 11*A*). In the presence of picrotoxin, the spike probability evoked by the first pulse was similar to that observed with the second pulse (Fig. 11*A*). Moreover, the facilitatory effect of picrotoxin was more pronounced during the SW− state (Fig. 11*B*). Thus, experimental conditions that favored the spike response of FSIs (see Fig. 10*B*) were those in which the effect of picrotoxin on MSNs was found to be larger (Fig. 11*A*,*B*). Finally, the enhancing effect of picrotoxin on spike probability was positively related to the stimulating current used to evoke spike responses in MSNs (ANOVA on linear regression, $r^2 = 0.34$; $F = 9.85$; $p = 0.0054$) (Fig. 11*C*).

Heterogeneous response probability during the SW+ state

Analysis of the striatal field potential during slow waves allowed us to discriminate two states: up and down states corresponded to the maximum and minimum of the field potential, respectively, and reflected depolarization and hyperpolarization of the membrane potential of MSNs (see above). However, it must be underlined that, regarding FSI, such a bimodal membrane potential has been observed *in vitro* (Plenz and Kitai, 1998) but not yet *in vivo*. Thus, cortical stimulation should be more efficient when occurring during membrane depolarization, i.e., during the up state. Indeed, we observed that the response probability of FSIs was >10 times higher during the up state than during the down state (Fig. 12). This higher probability during the up state was not observed regarding MSNs in the control condition but reappeared when MSNs were disinhibited by picrotoxin (Fig. 12). Therefore, this analysis further supports the view that FSIs strongly inhibit MSNs during the up state.

Discussion

FSIs form the most numerous class of GABAergic interneurons in the rat lateral striatum (Kawaguchi et al., 1995), but their role on striatal inhibition has not yet been investigated *in vivo*. In striatal slices, electrical stimulation evokes prominent $GABA_A$ postsynaptic responses (Lighthall and Kitai, 1983; Kita et al., 1985; Calabresi et al., 1991; Jiang and North, 1991; Kita, 1996). This $GABA_A$ inhibition of MSNs is mainly attributable to GABAergic interneurons (Kita, 1996; Plenz and Kitai, 1998; Koos and Tepper, 1999). However, *in vivo* experiments supporting a role of early $GABA_A$ inhibition in the striatum are scarce and controversial. Nisenbaum and Berger (1992) showed that local application of bicuculline decreased the threshold for spike discharge evoked by cortical stimulation, but Calabresi et al. (1990) and Wilson and Kawaguchi (1996) concluded that the postsynaptic potential evoked by cortical stimulation in MSNs has only a small $GABA_A$ component. We show here that FSIs can be distinguished *in vivo* from all other striatal neurons on the basis of electrophysiological criteria. Moreover, feedforward inhibition of MSNs by FSIs appears *in vivo* to play a major role in striatal integration of cortical information. This inhibition is effective because the spike response of FSIs occurs earlier and can be induced by a lower intensity of cortical stimulation than that required for MSNs.

Electrophysiological identification of striatal FSIs

FSIs exhibited two unique electrophysiological characteristics. First, their spike duration was shorter than that observed in all other striatal neurons. Second, FSIs were able to respond with bursts of three to five action potentials at 300 Hz to cortical stimulation. Both unique characteristics have been already observed *in vitro* (Kawaguchi, 1993; Kawaguchi et al., 1995; Plenz

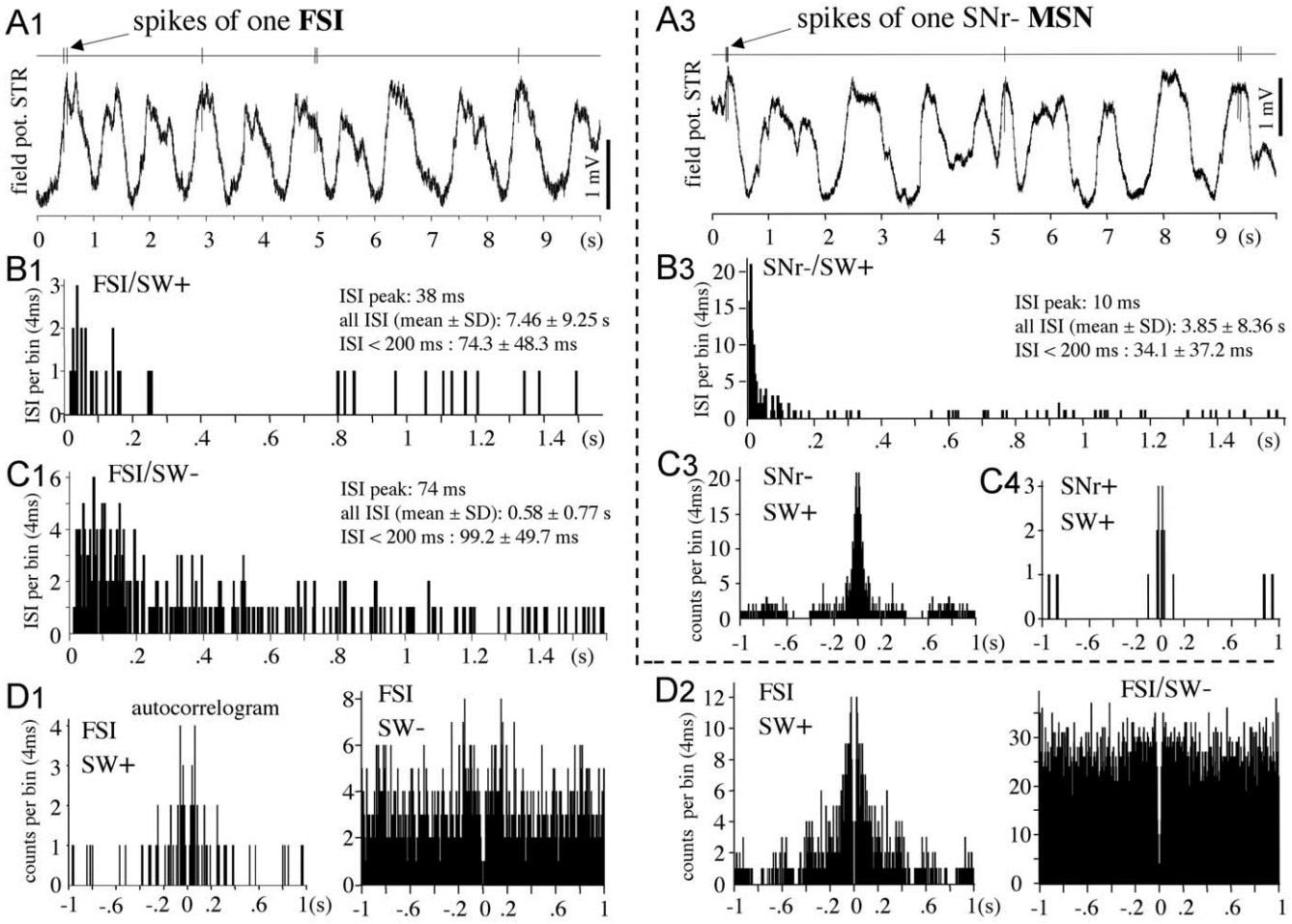

Figure 6. Spontaneous activity of FSIs and MSNs during both SW+ and SW− states. ***A1***, ***A3***, Simultaneous recordings of the striatal field potential with discharge activity of one FSI (***A1***) or one SNr− MSN (***A3***). ***B1***, ***C1***, The discharge activity of the FSI shown in ***A1*** was analyzed with ISI histograms (4 ms bins) calculated from recordings obtained in the SW+ state (***B1***; 125 spikes recorded in 930 s) and the SW− state (***C1***; 293 spikes recorded in 170 s). Notice the lack of an intermediate ISI (0.3–0.8 s range) during the SW+ state, denoting that FSIs only discharged during the upper state of the slow wave as exemplified in ***A1***. ***D1***, ***D2***, Autocorrelograms (4 ms bins) of the same FSI (***D1***) and of another, more active, FSI (***D2***) during both states. The central peaks observed in the SW+ state correspond to bursts occurring during the upper state of the slow waves. During the SW− state, autocorrelograms do not reveal any rhythmic activity. ***B3***, ISI histogram of the SNr− MSN illustrated in ***A3*** and recorded during the SW+ state (204 spikes recorded in 800 s). Because MSNs were completely silent or exhibited too low activity during the SW− state, this activity was not analyzed. ***C3***, Autocorrelogram of the same SNr− MSN shown in ***A3***. ***C4***, Autocorrelogram obtained from an SNr+ MSN exhibiting low activity (62 spikes recorded in 1670 s) during the SW+ state.

Table 2. Spontaneous firing of FSIs and of active MSNs during SW+ and SW− states

Parameter	MSN/SW+	FSI/SW+	FSI/SW−
Number of neurons	$n = 10$	$n = 8$	$n = 8$
Mean frequency (Hz)	0.209 ± 0.102	0.474 ± 0.129	3.67 ± 1.14*
(ISI <200 ms)/(all ISI) (%)	39.9 ± 4.3	34.7 ± 6.0	50.8 ± 8.6
Peak of ISI histograms (ms)	20.6 ± 3.2	24 ± 3.2	35.5 ± 6.9
Mean of all ISI(s)	7.39 ± 1.12**	3.62 ± 1.00	0.56 ± 0.16*
SD of all ISI(s)	11.42 ± 1.58***	4.41 ± 1.10	0.80 ± 0.28*
Mean of ISI <200 ms (ms)	38.8 ± 4.7**	64.0 ± 6.2	80.6 ± 5.8*
SD of ISI <200 ms (ms)	30.1 ± 3.2**	44.9 ± 4.2	47.6 ± 1.5

All MSNs studied were silent or exhibited an activity too low to be studied during the SW− state. Data were obtained from the spike analysis described in Figure 6. Values are expressed as mean ± SEM.

*Data obtained from eight FSIs during both states were compared with paired *t* tests, and statistically different observations are indicated in the right column (*$p < 0.02$).

,*Data obtained in 10 MSNs and eight FSIs during SW+ were compared with unpaired *t* tests, and statistically different observations are indicated in the left column (**$p < 0.05$; ***$p < 0.01$).

and Kitai, 1998; Koos and Tepper, 1999). All neurons exhibiting such characteristics and injected with neurobiotin were parvalbumin-positive. Thus, our electrophysiological criteria were sufficient to identify FSIs.

Experimental conditions favoring FSI activity are associated with inhibition of MSNs

We observed that, during the SW+ state, corticostriatal neurons and MSNs discharged synchronously with the positive phase of cortical field potential. This is consistent with previous studies showing that MSNs discharge only during the up state (Wilson and Groves, 1981; Wilson, 1993; Wilson and Kawaguchi, 1996) and that MSN activity is correlated with cortical slow waves and corticostriatal activity (Mahon et al., 2001; Tseng et al., 2001; Kasanetz et al., 2002). FSIs exhibited the same discharge pattern, but their discharge rate was much higher than that of MSNs. Plenz and Kitai (1998) also observed in organotypic cultures that, like MSNs, FSIs exhibit membrane potential oscillations and are more active than MSNs during the up state. Moreover, we observed that MSNs preferentially discharge before the maximum of the striatal slow wave, whereas the activity of corticostriatal neurons and of FSIs was more widely distributed and centered close to cortical and striatal waves, respectively. This is consistent with the findings of Mahon et al. (2001), who have observed that MSNs preferentially discharge during the initial part of the up state. Therefore, MSNs become silent during the up state when

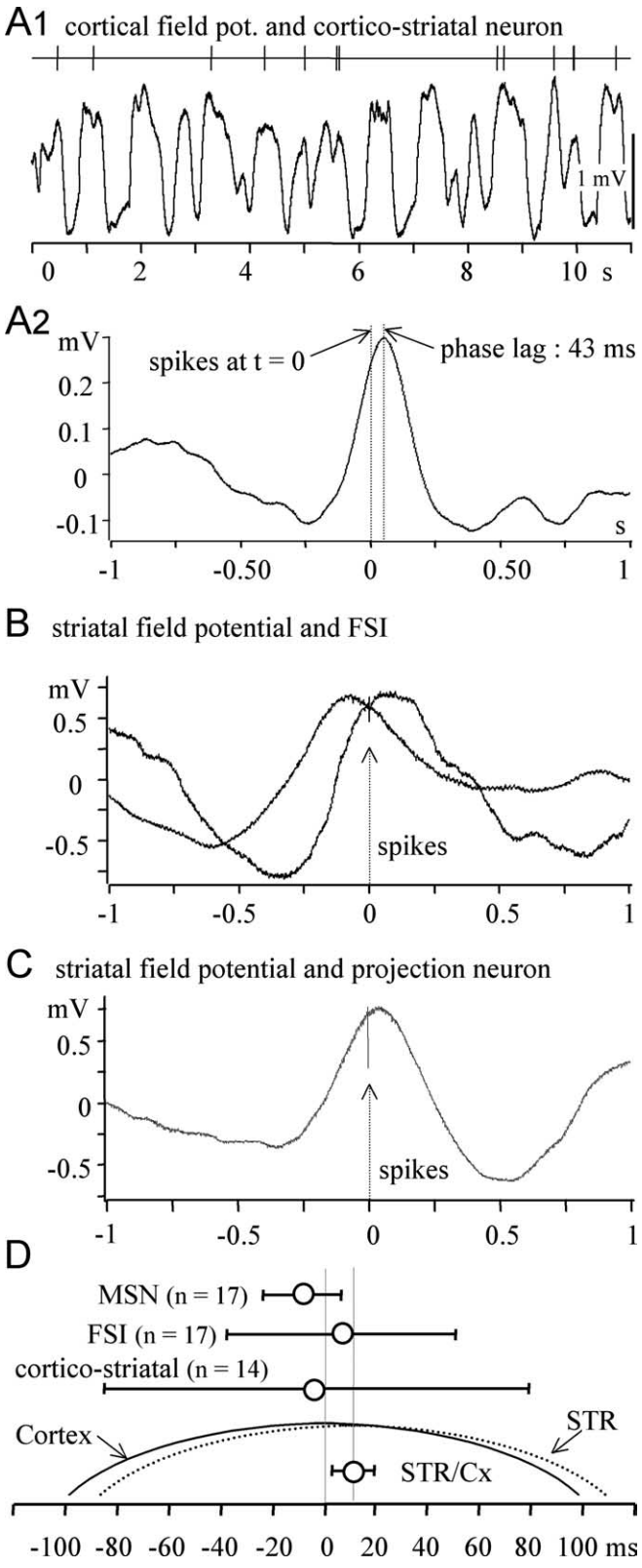

Figure 7. Temporal relationship between discharge activity and slow waves. ***A1***, The discharge activity of one corticostriatal neuron was recorded together with the cortical field potential. ***A2***, Sections of field potential recordings centered on every spike were averaged together (same neuron as in ***A1***, 287 spikes recorded during a continuous period of an SW+ state lasting for 270 s). This averaged recording shows that this cortical neuron discharged, on average, 43 ms before the maximum of the cortical slow wave. ***B***, Two examples of averaged striatal field potential recordings centered on every spike of two FSIs. One FSI discharged before the maximum of the wave (12 spikes recorded in 300 s), and another FSI (recording illustrated in Fig. 4) discharged after the maximum (76 spikes recorded in 120 s). ***C***, Averaged field potential recording centered on spikes of one SNr− MSN (recording illustrated in Fig. 6*B3*; 204 spikes recorded within 810 s). ***D***, Temporal relationship between the slow waves and the discharge activity of the three neuronal groups (numbers indicated in parentheses). The bars indicate the mean ± SD. All neurons discharged closely to the maximum of the slow wave. Notice, however, that MSNs tended to discharge before the maximum of the striatal (STR) wave.

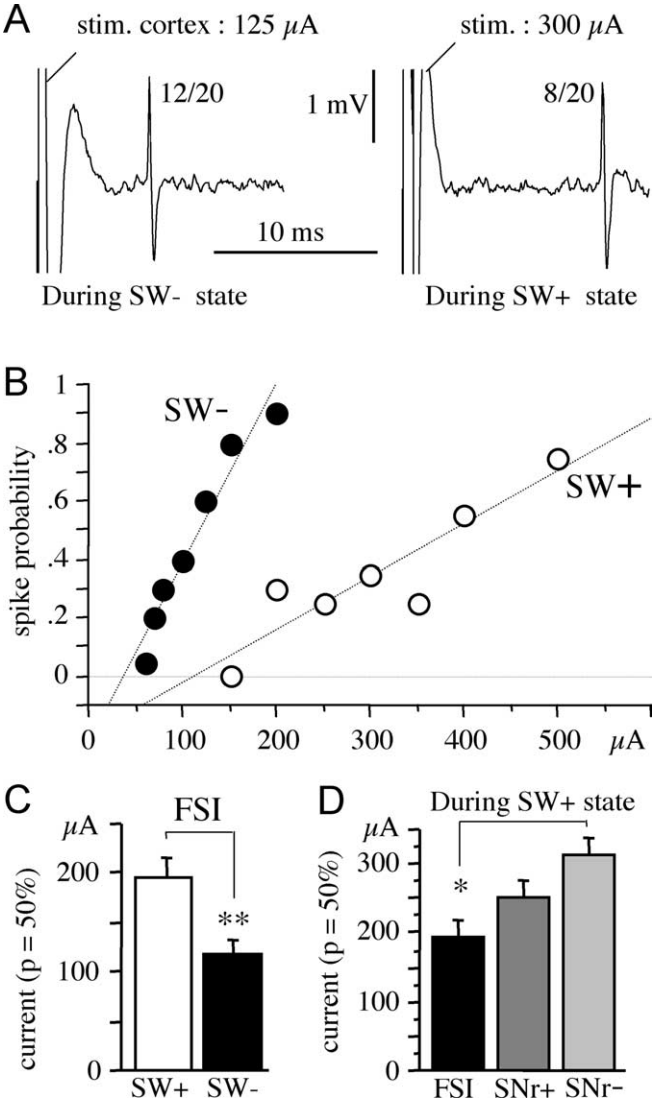

Figure 8. Relationship between the discharge probability of FSIs and the amplitude of cortical stimulation. ***A***, The discharge probability was estimated from the number of spikes evoked by a series of 20 cortical stimulations (stim.) applied every 3 s at a fixed current. The same cell was tested both in SW+ and SW− states asserted by simultaneous recording of the striatal field potential (data not shown). ***B***, Summary of the discharge probability of the FSI shown in ***A*** plotted versus the stimulating current. ***C***, From the relationship shown in ***B***, the stimulating current necessary to evoke spike responses with a 50% probability was estimated for 11 FSIs during both states. ***D***, during the SW+ state, the current necessary to evoke spikes with a 50% probability was compared for 11 FSIs with that for 22 SNr+ neurons and for 24 SNr− neurons. Histograms show the mean ± SEM (**$p < 0.001$; *$p < 0.01$). FSIs were more responsive to cortical stimulation than MSNs during the SW+ state and were more responsive during the SW− state than during the SW+ state.

FSIs reach their maximal activity. Thus, FSIs might contribute to reduce the discharge probability of MSNs during the up state. During cortical desynchronization, FSIs are more active, whereas MSNs are less active, compared with the SW+ state. Moreover, a

←

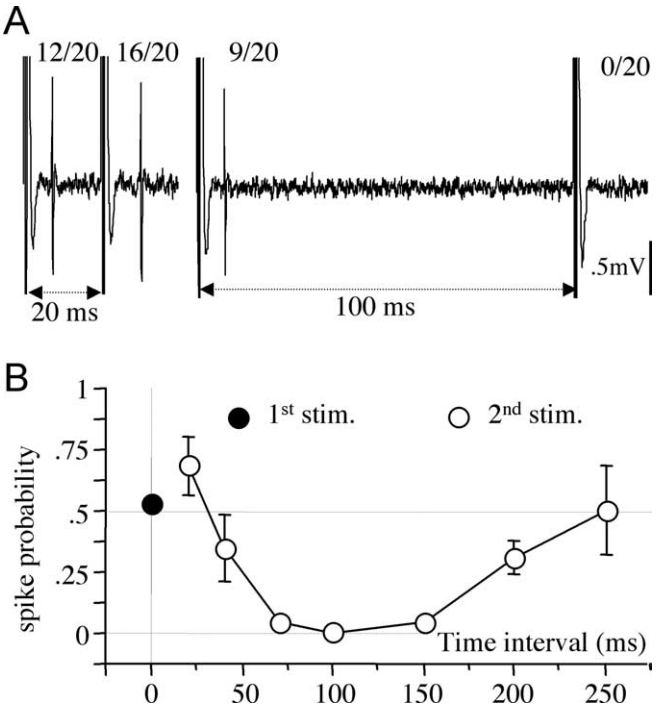

Figure 9. Spike responses of FSI to paired cortical stimulation at variable time intervals. ***A***, Twenty consecutive pairs of cortical stimulations were applied every 3 s for each time interval. The stimulating current was adjusted with preliminary tests to evoke a discharge probability to the first stimulation close to 50% and was not further modified. ***B***, The discharge probability in response to the second pulse was tested for seven distinct time intervals either in the SW− state (6 FSIs) or in the SW+ state (3 FSIs). Because the cortical state did not influence the relative spike probability in response to the second pulse compared with the first at any time interval, data were pooled. Bars indicate the mean ± SEM. stim., Stimulation.

tail pinch disrupted slow waves and always triggered a burst in FSIs, whereas MSN activity was inhibited. These observations suggest that FSIs might inhibit MSNs during the SW− state and sensorial stimuli.

The striatal down state, indirectly monitored here by field potential recording, corresponds to a hyperpolarized state of MSNs caused by a rhythmic depression of cortical activity (Wilson, 1993). The fact that FSIs were silent and less responsive to cortical stimulation during this down state suggests that, like MSNs, they were hyperpolarized. The same mechanism might also explain the paired pulse disfacilitation observed in FSI responses. Indeed, Wilson et al. (1983) showed that cortical stimulation induced a long-lasting (100–300 ms) hyperpolarization of MSNs. They demonstrated that this hyperpolarization was not caused by an intrastriatal GABAergic synaptic mechanism but by "an identical period of active inhibition of cortical neurons." This electrically evoked cortical inhibition was also observed in our experimental conditions. Therefore, it is likely that every cortical stimulation induced, in the corresponding striatum, an artificial down state, which disfacilitated the spike response of both FSIs and MSNs to a second stimulation triggered 100 ms after the first. The likely similarity between FSIs and MSNs regarding their membrane potential oscillations might also explain why the SW− state facilitated the spontaneous activity and spike response probability of FSIs. Indeed, MSNs exhibited a sustained membrane potential close to their up state when the SW+ state was disrupted by a tail pinch (Kasanetz et al., 2002), and we observed that corticostriatal neurons exhibited regularly spaced activity during the SW− state. This tonic cortical activity might maintain FSIs in a depolarized state, thus facilitating their spike discharge.

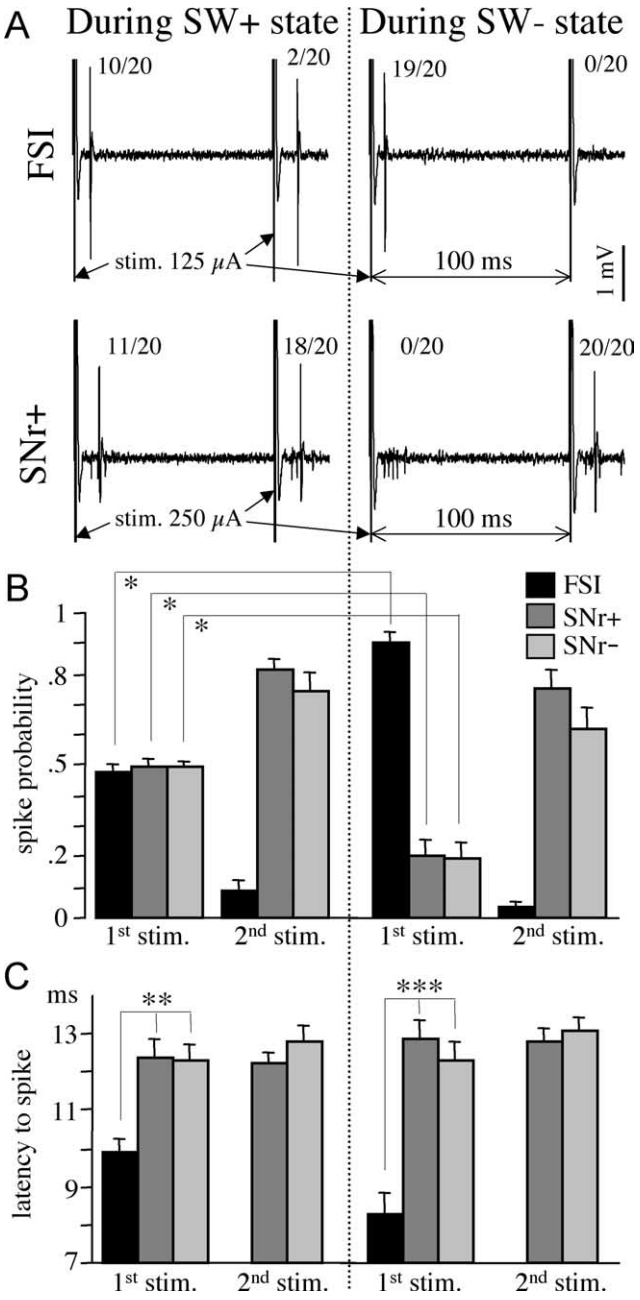

Figure 10. Discharge probability and spike latency of FSIs and MSNs to paired cortical stimulation. ***A***, To test every discharge probability, pairs of cortical stimulation (stim.; 100 ms interval) were applied 20 times every 3 s. For every individual neuron, the stimulating current was adjusted by preliminary tests so that the discharge responses evoked by the first pulse during the SW+ state exhibited a 50% probability. Then this stimulating current was used to test every individual neuron in both states. Typical recordings illustrate the spike responses of one FSI and of one SNr+ neuron recorded in the same rat. ***B***, Discharge probability of 11 FSIs and 22 SNr+ and 24 SNr− neurons. The discharge probabilities in response to the first pulse observed in both states significantly differed for the three groups (paired *t* test, $*p < 0.0001$). ***C***, From individual recordings as illustrated in ***A***, the latency (i.e., the time interval between stimulation pulse and evoked spike) was measured. However, the spike latency of FSIs to the second pulse was not shown because of the low number of spikes. Regarding the response to the first pulse, the spike latency of FSIs was compared with that of SNr+ and SNr− neurons in both cortical states (unpaired *t* test; $**p < 0.002$; $***p < 0.0001$). Bar histograms indicate mean ± SEM.

Experimental conditions that depolarize MSNs and, probably, FSIs (spontaneous up state and SW− state), should facilitate their spike response to cortical stimulation, whereas those that hyperpolarize them (spontaneous and electrically evoked down

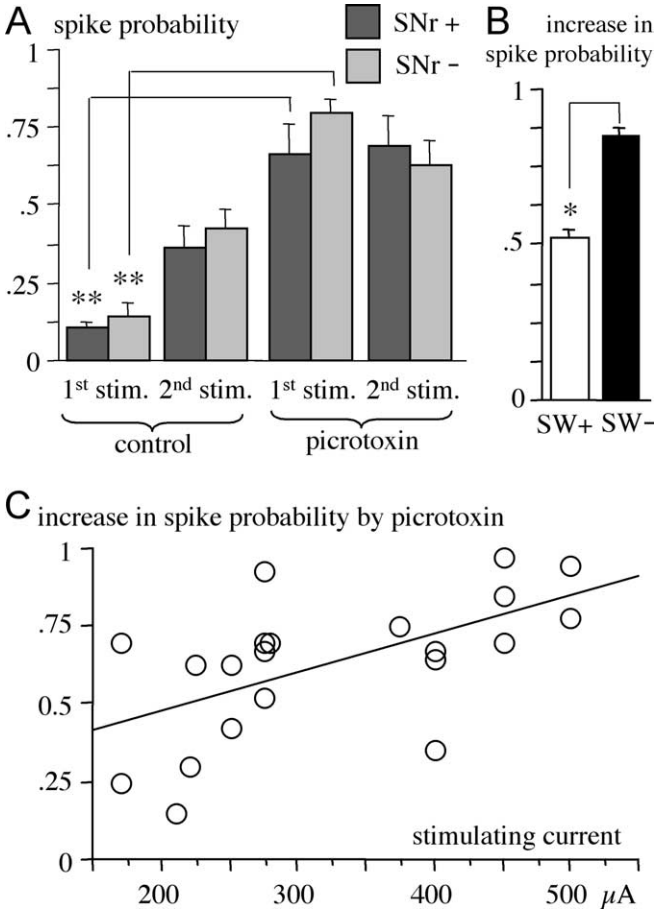

Figure 11. Effects of local picrotoxin injection on the discharge probability of MSNs. ***A***, The discharge probability of 10 SNr+ neurons and 11 SNr− neurons was tested, as illustrated in Fig. 10*A*, with paired cortical stimulation (stim.; 100 ms interval) applied every 3 s. Forty control stimulations were applied just before pressure injection of picrotoxin (1 mM, 20–30 nl) 150 μm above every recorded cell. Then the spike responses to 40 paired stimulations were recorded between 1 and 3 min after picrotoxin injection. The stimulating current was adjusted for every individual neuron by means of preliminary tests so that the spike responses to the second pulse exhibited a probability close to 40% in control conditions. Only experiments during which the cortical state remained stable were considered. Picrotoxin injection significantly enhanced the spike probability evoked by the first pulse (**$p < 0.001$). ***B***, In two SNr+ and three SNr− neurons (data pooled), the effect of picrotoxin was tested in both SW+ and SW− states. The histogram shows that the enhancing effect of picrotoxin on the spike probability in response to the first pulse was larger during the SW− state (*$p < 0.005$). Bar histograms show the mean ± SEM. ***C***, For the 21 MSNs studied, the enhancing effect of picrotoxin on spike probability in response to the first pulse was indicated as a function of the stimulating current.

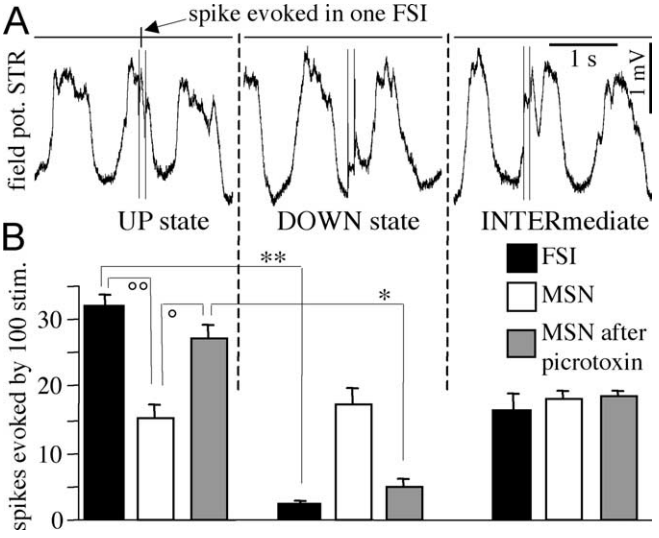

Figure 12. The discharge probability in response to cortical stimulation depends on its occurrence during distinct states of the slow waves. Series of 20 consecutive paired cortical stimulations were applied every 3 s. In this analysis, only the response to the first pulse was considered. The striatal (STR) field potential allowed us to distinguish between three states: up and down states corresponded to the maximum and minimum of the field potential, respectively (***A***). Recording periods that did not clearly fall in either state were classified as intermediate. Each observation corresponded to the number of evoked spikes in all three states in response to groups of 100 stimulations. These groups were obtained by pooling data from four or five neurons. Six groups were obtained from 22 FSIs, and six groups were obtained from 30 MSNs. Four groups were obtained from 14 MSNs recorded 3–6 min after picrotoxin injection. The stimulating current was adjusted by preliminary tests so that the response probability to the first pulse was close to 50%. Thus, regarding the 14 MSNs tested before and after picrotoxin, the stimulating current used for recordings under picrotoxin influence was decreased (on average by 61 μA) in comparison with that used before picrotoxin injection. Bar histograms show means ± SEM. Statistically significant differences were demonstrated by paired *t* test (*$p < 0.005$; **$p < 0.0001$) or unpaired *t* test (°$p < 0.01$; °°$p < 0.001$). Notice that both FSIs and MSNs that were recorded under picrotoxin influence preferentially discharged during the up state. However, in control conditions, MSNs did not show such a preference, suggesting that their spike response evoked during the up state was actually inhibited by that of FSIs.

state), should have inhibitory consequences on both neuronal types. We actually observed the expected facilitation and disfacilitation of FSI responses but reverse effects on MSN responses. This reverse correlation suggests that FSIs can exert a powerful feedforward inhibition on MSNs *in vivo*, as suggested by *in vitro* studies (Plenz and Kitai, 1998; Koos and Tepper, 1999).

Feedforward inhibition of MSNs by FSIs

To further demonstrate that FSIs do inhibit MSNs, we showed that (1) FSIs are more sensitive to cortical input than MSNs; (2) their spike response occurs earlier than that of MSNs; and (3) blockade of $GABA_A$ receptors suppresses MSN inhibition. First, on average, the stimulating current necessary to evoke spikes by cortical stimulation was lower for FSIs than for MSNs, and this difference was more pronounced during the SW− state, which favors the FSI response. Our observation is consistent with that of Parthasarathy and Graybiel (1997): cortical stimulation induced a more pronounced increase of Fos protein in parvalbumin-positive cells than in other striatal neurons.

Second, spike responses evoked by cortical stimulation occurred earlier for FSIs than for MSNs: regarding striatonigral neurons, the latency difference reached 4.6 ms during the SW− state. This difference is compatible with the kinetics of the inhibitory synapses formed by FSIs on MSNs. Indeed, simultaneous recording of FSIs and MSNs have been performed in organotypic cultures (Plenz and Kitai, 1998) and in striatal slices (Koos and Tepper, 1999; Koos et al., 2004). Single FSI spikes evoked rapid postsynaptic responses in MSNs, which reached at least 60% of their maximum within 4.6 ms. These rapid kinetics have already been reported regarding several synapses formed by GABAergic interneurons in other brain areas (Jonas et al., 2004) and are consistent with anatomical observations: parvalbumin-positive synapses on MSNs are mainly located on somata and proximal dendrites (Bennett and Bolam, 1994).

Third, blocking $GABA_A$ receptors by local picrotoxin enhanced the probability of spike discharge evoked in MSNs by cortical stimulation. The characteristics of this increase further revealed a specific inhibition by FSIs. Indeed, experimental conditions favoring FSI activity (SW− state and responses evoked by the first pulse in a pair) were associated with a larger enhancing effect of picrotoxin. Moreover, during the SW+ state, FSIs pref-

erentially responded to cortical stimulation during the up state, and picrotoxin restored the same preferential response in MSNs.

In our experimental conditions, lateral inhibition of MSNs by themselves was probably weak compared with feedforward inhibition by GABA interneurons. First, because most MSNs were silent, especially during the SW− state, GABA inhibition by spontaneous MSN activity is negligible. Second, regarding the responses evoked by the first pulse in a pair, it is unlikely that early responsive MSNs were able to inhibit late responses because the spike responses evoked by cortical stimulation in MSNs occurred with a relatively constant latency independent of spike probability. Third, in paired pulse stimulations, it is unlikely that spike responses of MSNs to the first pulse could inhibit the response to the second pulse. Indeed, the IPSP evoked in one MSN by an action potential in another MSN lasts for ~40 ms (Czubayko and Plenz 2002; Tunstall et al., 2002; Koos et al., 2004), whereas we used here a paired-pulse interval of 100 ms. Fourth, although MSNs were more responsive to the second than to the first pulse in a paired-pulse stimulation, the enhancing effect of picrotoxin was larger regarding the response to the first than to the second pulse. These considerations lead to the conclusion that, in our experimental conditions, striatal GABA inhibition is mainly attributable to GABAergic interneurons, among which FSIs play a prominent role in the rostrolateral striatum.

Functional significance and physiopathological consequences

We showed that FSIs preferentially inhibit weak corticostriatal inputs. Indeed, although most MSNs were less sensitive than FSIs to cortical stimulation, a few MSNs were actually more sensitive. Moreover, picrotoxin, which reveals GABA inhibition by FSIs in our experimental conditions, more strongly affected MSNs that exhibited the lowest sensitivity to cortical stimulation. Thus, feedforward inhibition by FSIs filters cortical information effectively transmitted by striatal projection neurons.

The slow-wave activity, which resembles slow-wave sleep, is caused by synchronous activity of cortical neurons (Steriade, 2000). Although this rhythmic activity induces membrane potential oscillations in MSNs, their discharge activity remains low during these oscillations. We suggest that FSIs might contribute to this low discharge probability. Likewise, during absence seizures in rats, cortical neurons discharge rhythmically at 7 Hz and generate large-amplitude oscillations in MSN membrane potential. However, the mean discharge activity of MSNs was actually reduced during absence seizures, whereas the activity of GABAergic interneurons was dramatically increased (Slaght et al., 2004). These authors suggested that, during seizures, the discharge of MSNs was suppressed via feedforward inhibition by GABAergic interneurons. It is interesting to note that in both cases (slow-wave sleep and absence seizures), intense rhythmic activity in the cortex, associated with movement inhibition, is correlated with a blockade of the cortical information at the level of the striatum, the main input structure of the basal ganglia.

FSIs are excited by dopamine (Bracci et al., 2002; Centonze et al., 2003), and the discharge activity of MSNs is increased by dopaminergic denervation (Tseng et al., 2001). Our study suggests a link between both observations: dopaminergic lesions might diminish the response of FSIs to cortical inputs and, thus, might release MSNs from normal feedforward inhibition. Therefore, disregulation of FSIs might play a major role in the cognitive and motor deficits associated with Parkinson's disease.

References

Bennett BD, Bolam JP (1994) Synaptic input and output of parvalbumin-immunoreactive neurons in the neostriatum of the rat. Neuroscience 62:707–719.

Berke JD, Okatan M, Skurski J, Eichenbaum HB (2004) Oscillatory entrainment of striatal neurons in freely moving rats. Neuron 43:883–896.

Bolam JP, Hanley JJ, Booth PA, Bevan MD (2000) Synaptic organisation of the basal ganglia. J Anat 196:527–542.

Bracci E, Centonze D, Bernardi G, Calabresi P (2002) Dopamine excites fast-spiking interneurons in the striatum. J Neurophysiol 87:2190–2194.

Calabresi P, Mercuri NB, Stefani A, Bernardi G (1990) Synaptic and intrinsic control of membrane excitability of neostriatal neurons. I. An in vivo analysis. J Neurophysiol 63:651–662.

Calabresi P, Mercuri NB, De Murtas M, Bernardi G (1991) Involvement of GABA systems in feedback regulation of glutamate-and GABA-mediated synaptic potentials in rat neostriatum. J Physiol (Lond) 440:581–599.

Centonze D, Grande C, Usiello A, Gubellini P, Erbs E, Martin AB, Pisani A, Tognazzi N, Bernardi G, Moratalla R, Borrelli E, Calabresi P (2003) Receptor subtypes involved in the presynaptic and postsynaptic actions of dopamine on striatal interneurons. J Neurosci 23:6245–6254.

Cowan RL, Wilson CJ, Emson PC, Heizmann CW (1990) Parvalbumin-containing GABAergic interneurons in the rat neostriatum. J Comp Neurol 302:197–205.

Czubayko U, Plenz D (2002) Fast synaptic transmission between striatal spiny projection neurons. Proc Natl Acad Sci USA 99:15764–15769.

Deniau JM, Menetrey A, Charpier S (1996) The lamellar organization of the rat substantia nigra pars reticulata: segregated patterns of striatal afferents and relationship to the topography of corticostriatal projections. Neuroscience 73:761–781.

Figueredo-Cardenas G, Medina L, Reiner A (1996) Calretinin is largely localized to a unique population of striatal interneurons in rats. Brain Res 709:145–150.

Gerfen CR, Wilson CJ, eds (1996) The basal ganglia. Amsterdam: Elsevier.

Goto Y, O'Donnell P (2001) Network synchrony in the nucleus accumbens *in vivo*. J Neurosci 21:4498–4504.

Graybiel AM (1995) Building action repertoires: memory and learning functions of the basal ganglia. Curr Opin Neurobiol 5:733–741.

Jaeger D, Kita H, Wilson CJ (1994) Surround inhibition among projection neurons is weak or nonexistent in the rat neostriatum. J Neurophysiol 72:2555–2558.

Jiang ZG, North RA (1991) Membrane properties and synaptic responses of rat striatal neurones in vitro. J Physiol (Lond) 443:533–553.

Jonas P, Bischofberger J, Fricker D, Miles R (2004) Interneuron diversity series: fast in, fast out-temporal and spatial signal processing in hippocampal interneurons. Trends Neurosci 27:30–40.

Kasanetz F, Riquelme LA, Murer MG (2002) Disruption of the two-state membrane potential of striatal neurones during cortical desynchronisation in anaesthetised rats. J Physiol (Lond) 543:577–589.

Kawaguchi Y (1993) Physiological, morphological, and histochemical characterization of three classes of interneurons in rat neostriatum. J Neurosci 13:4908–4923.

Kawaguchi Y, Wilson CJ, Augood SJ, Emson PC (1995) Striatal interneurones: chemical, physiological and morphological characterization. Trends Neurosci 18:527–535.

Kita H (1993) GABAergic circuits of the striatum. Prog Brain Res 99:51–72.

Kita H (1996) Glutamatergic and GABAergic postsynaptic responses of striatal spiny neurons to intrastriatal and cortical stimulation recorded in slice preparations. Neuroscience 70:925–940.

Kita H, Kosaka T, Heizmann CW (1990) Parvalbumin-immunoreactive neurons in the rat neostriatum: a light and electron microscopic study. Brain Res 536:1–15.

Kita T, Kita H, Kitai ST (1985) Local stimulation induced GABAergic response in rat striatal slice preparations: intracellular recordings on QX-314 injected neurons. Brain Res 360:304–310.

Koos T, Tepper JM (1999) Inhibitory control of neostriatal projection neurons by GABAergic interneurons. Nat Neurosci 2:467–472.

Koos T, Tepper JM, Wilson CJ (2004) Comparison of IPSCs evoked by spiny and fast-spiking neurons in the neostriatum. J Neurosci 24:7916–7922.

Lighthall JW, Kitai ST (1983) A short duration GABAergic inhibition in identified neostriatal medium spiny neurons: in vitro slice study. Brain Res Bull 11:103–110.

Luk KC, Sadikot AF (2001) GABA promotes survival but not proliferation of parvalbumin-immunoreactive interneurons in rodent neostriatum: an in vivo study with stereology. Neuroscience 104:93–103.

Mahon S, Deniau JM, Charpier S (2001) Relationship between EEG potentials and intracellular activity of striatal and cortico-striatal neurons: an in vivo study under different anesthetics. Cereb Cortex 11:360–373.

McGeorge AJ, Faull RLM (1989) The organization of the projection from the cerebral cortex to the striatum in the rat. Neuroscience 29:503–537.

Nisenbaum ES, Berger TW (1992) Functionally distinct subpopulations of striatal neurons are differentially regulated by GABAergic and dopaminergic inputs—I. In vivo analysis. Neuroscience 48:561–578.

Parthasarathy HB, Graybiel AM (1997) Cortically driven immediate-early gene expression reflects modular influence of sensorimotor cortex on identified striatal neurons in the squirrel monkey. J Neurosci 17:2477–2491.

Paxinos G, Watson C (1997) The rat brain in stereotaxic coordinates. London: Academic.

Pinault D (1996) A novel single-cell staining procedure performed in vivo under electrophysiological control: morpho-functional features of juxtacellularly labeled thalamic cells and other central neurons with biocytin or Neurobiotin. J Neurosci Methods 65:113–136.

Plenz D (2003) When inhibition goes incognito: feedback interaction between spiny projection neurons in striatal function. Trends Neurosci 26:436–443.

Plenz D, Kitai ST (1998) Up and down states in striatal medium spiny neurons simultaneously recorded with spontaneous activity in fast-spiking interneurons studied in cortex-striatum-substantia nigra organotypic cultures. J Neurosci 18:266–283.

Ramanathan S, Hanley JJ, Deniau JM, Bolam JP (2002) Synaptic convergence of motor and somatosensory cortical afferents onto GABAergic interneurons in the rat striatum. J Neurosci 22:8158–8169.

Ryan LJ, Young SJ, Groves PM (1986) Substantia nigra stimulation evoked antidromic responses in rat neostriatum. Exp Brain Res 63:449–460.

Schultz W, Tremblay L, Hollerman JR (2003) Changes in behavior-related neuronal activity in the striatum during learning. Trends Neurosci 26:321–328.

Slaght SJ, Paz T, Chavez M, Deniau JM, Mahon S, Charpier S (2004) On the activity of the corticostriatal networks during spike-and-wave discharges in a genetic model of absence epilepsy. J Neurosci 24:6816–6825.

Steriade M (2000) Corticothalamic resonance, states of vigilance and mentation. Neuroscience 101:243–276.

Stern EA, Kincaid AE, Wilson CJ (1997) Spontaneous subthreshold membrane potential fluctuations and action potential variability of rat corticostriatal and striatal neurons in vivo. J Neurophysiol 77:1697–1715.

Tseng KY, Kasanetz F, Kargieman L, Riquelme LA, Murer MG (2001) Cortical slow oscillatory activity is reflected in the membrane potential and spike trains of striatal neurons in rats with chronic nigrostriatal lesions. J Neurosci 21:6430–6439.

Tunstall MJ, Oorschot DE, Kean A, Wickens JR (2002) Inhibitory interactions between spiny projection neurons in the rat striatum. J Neurophysiol 88:1263–1269.

Wilson CJ (1987) Morphology and synaptic connections of crossed corticostriatal neurons in the rat. J Comp Neurol 263:567–580.

Wilson CJ (1993) The generation of natural firing patterns in neostriatal neurons. Prog Brain Res 99:277–297.

Wilson CJ, Groves PM (1981) Spontaneous firing patterns of identified spiny neurons in the rat neostriatum. Brain Res 220:67–80.

Wilson CJ, Kawaguchi Y (1996) The origins of two-state spontaneous membrane potential fluctuations of neostriatal spiny neurons. J Neurosci 16:2397–2410.

Wilson CJ, Chang HT, Kitai ST (1983) Disfacilitation and long-lasting inhibition of neostriatal neurons in the rat. Exp Brain Res 51:227–235.

Wilson CJ, Chang HT, Kitai ST (1990) Firing patterns and synaptic potentials of identified giant aspiny interneurons in the rat neostriatum. J Neurosci 10:508–519.

Wu Y, Parent A (2000) Striatal interneurons expressing calretinin, parvalbumin or NADPH-diaphorase: a comparative study in the rat, monkey and human. Brain Res 863:182–191.